

Dynamic Pyramid Network for Efficient Multimodal Large Language Model

Hao Ai¹, Kunyi Wang³, Zezhou Wang³, Hao Lu⁴, Jin Tian³, Yixin Luo⁵
 Peng Xing⁶, Jen-Yuan Huang⁷, Huaxia Li⁸, Gen Luo²

¹BeiHang University ²Shanghai AI Laboratory ³KAUST

⁴Hong Kong University of Science and Technology (Guangzhou) ⁵Technical University Of Denmark
⁶Nanjing University of Science and Technology ⁷Peking University ⁸Xiaohongshu Inc

Abstract

Multimodal large language models (MLLMs) have demonstrated impressive performance in various vision-language (VL) tasks, but their expensive computations still limit the real-world application. To address this issue, recent efforts aim to compress the visual features to save the computational costs of MLLMs. However, direct visual compression methods, e.g. efficient projectors, inevitably destroy the visual semantics in MLLM, especially in difficult samples. To overcome this shortcoming, we propose a novel dynamic pyramid network (DPN) for efficient MLLMs. Specifically, DPN formulates MLLM as a hierarchical structure where visual features are gradually compressed with increasing depth. In this case, even with a high compression ratio, fine-grained visual information can still be perceived in shallow layers. To maximize the benefit of DPN, we further propose an innovative Dynamic Pooling Experts (DPE) that can dynamically choose the optimal visual compression rate according to input features. With this design, harder samples will be assigned larger computations, thus preserving the model performance. To validate our approach, we conduct extensive experiments on two popular MLLMs and ten benchmarks. Experimental results show that DPN can save up to 56% average FLOPs on LLaVA while further achieving +0.74% performance gains. Besides, the generalization ability of DPN is also validated on the existing high-resolution MLLM called LLaVA-HR. Our source codes are anonymously released at <https://github.com/aihao2000/DPN-LLaVA>

1. Introduction

Multimodal large language models (MLLMs) have achieved significant progress in computer vision [9–11, 20, 24, 27, 29, 33, 48], which continuously breakthroughs the performance limit of various vision-language (VL) tasks [12–14, 19, 23, 30, 32, 40, 50, 51]. Among them, the mainstream paradigm is to insert visual tokens

from pre-trained encoder into the LLM, and then fine-tune the entire MLLM. Despite effectiveness, expensive computation remains the main bottleneck of existing MLLMs in real-world applications [6, 46], especially when image resolutions greatly increase [33].

To address this issue, increasing efforts are devoted to the efficient MLLM architectures [6, 10, 11, 26, 45]. Among them, MoE-based approaches [26] aim to reduce the activated parameters of MLLMs via the mixture of expert, thereby improving the efficiency. However, these methods typically require expensive training stages for their MoE-based learning. Recently, another cheap and promising trend is to reduce the visual tokens of MLLMs via the efficient visual projector [2, 10, 22, 38]. For instance, Resampler [2] compresses visual features into few learnable tokens via the cross-attentions. By placing it before the LLM, the computation costs of MLLMs can be obviously saved due to the reduction of input sequence.

Despite the efficiency, we identify that these methods are sub-optimal and often sacrifice the visual representation. Specifically, most existing visual projectors are typically placed outside the LLM and downsample visual features via their saliency [10, 22]. Such straightforward practice ignores the visual semantics and the textual prompt, thus easily destroying the fine-grained visual content, e.g., OCR words and small objects. More importantly, all samples are aligned with the same visual compression rate, e.g., 75% for 2×2 pooling, which inevitably hurts the understanding of hard samples and leads to the redundant computation on easy samples.

To overcome this shortcoming, we argue that the MLLM should be designed as a pyramid structure, in which visual compression modules, e.g., pooling layers, are embedded into LLM in a hierarchical manner. In this way, visual information is mostly preserved in the shallow layers of LLM for fine-grained perception and gradually compressed in deeper layers for high-level understanding. Compared to previous works [6, 10, 22, 38, 45], even with a high compression rate, MLLM can still capture critical visual content for vision-

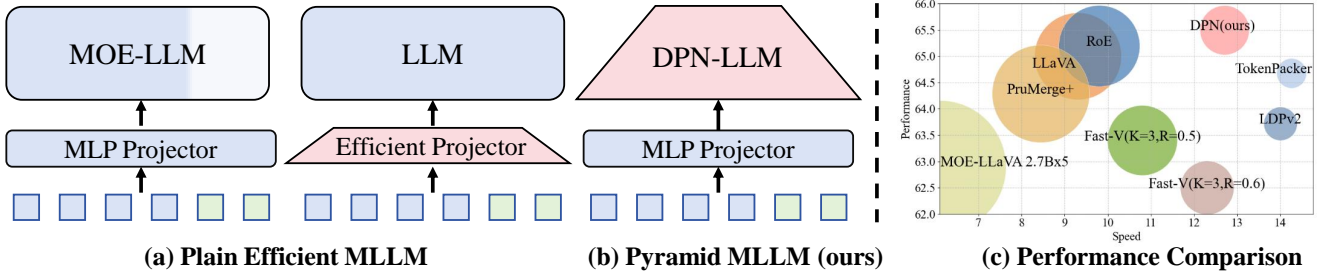


Figure 1. **Illustration of existing plain MLLMs with our dynamic pyramid network (DPN).** Compared to plain MLLMs, our DPN can dynamically compress the input tokens in a hierarchical manner while greatly preventing the model performance.

language understanding. Besides, such hierarchical structure is also aligned with the most successful design principle in computer vision, *e.g.*, Swin-Transformer [31].

Based on the above principle, we propose a novel dynamic pyramid network for MLLMs, namely (DPN). As shown in Fig. 2, DPN not only adopts a pyramid structure to realize effective visual compression, but can also dynamically adjust the compression rate based on samples. To approach this target, DPN is equipped with a set of dynamic pooling experts (DPE), which aim to select an optimal pooling rate based on input features. To maximize the benefits of DPE, we propose a novel routing loss to encourage visual sparsity while preserving performance. With these designs, DPN can be seamlessly deployed on existing MLLMs without additional training stages.

To validate our approach, we adopt DPN to two popular MLLMs, *i.e.*, LLaVA [29] and LLaVA-HR [33], and conduct extensive experiments on 10 MLLM benchmarks, *e.g.*, MM-Vet [50]. Experiments not only confirm the great efficiency of DPN against existing methods, but also validate its competitive performance compared to the baseline. For example, compared to LLaVA-HR-X [33], our DPN-LLaVA-HR-X achieves 1.4 \times speedup and +0.62% performance gains. In conclusion, our contributions can be summarized in three folds:

- We propose a novel Dynamic Pyramid Network (DPN) for multimodal large language models (MLLMs), which can achieve significant inference acceleration with minor performance sacrifice.
- In DPN, we propose an innovative Dynamic Pooling Experts (DPE) that can dynamically choose the optimal visual pooling rate based on input features. DPE is also equipped with a routing loss to maximize its benefits during training.
- Compared to existing methods, DPN reduces up to 56% average Flops on 10 benchmarks, while also well preserving the model performance, *e.g.*, +0.74 gains on LLaVA.

2. Related Work

2.1. Pyramid Network

Pyramid-based networks have demonstrated exceptional performance across various traditional tasks, including detection and segmentation. One such network, the Feature Pyramid Network (FPN) [28], leverages the inherent multi-scale, pyramidal hierarchy of deep convolutional networks to construct feature pyramids at a marginal additional cost. The FPN architecture utilizes a top-down approach with lateral connections to produce high-level semantic feature maps across multiple scales, which significantly enhances its utility as a generic feature extractor in numerous applications. The concept of this pyramid-shaped network has been carried forward into the era of transformers[42]. The Pyramid Vision Transformer (PVT)[44] integrates a progressive pyramid structure to reduce the computational burden of processing large feature maps. By combining the strengths of both convolutional neural networks (CNNs)[36] and transformers, PVT has achieved superior performance in downstream tasks such as object detection and instance segmentation.

2.2. Multimodal Large Language Models

With the rise of large language models (LLMs)[1, 8, 15, 35, 41, 49], an increasing number of researchers have turned their attention to the construction of multimodal large language models. The primary approach for extending LLMs into multimodal large language models (MLLMs) [9–11, 20, 24, 27, 29, 33, 43, 48] is connecting pre-trained image encoders, such as CLIP[37], aligning image and text features, and fine-tuning on visual question answering tasks. For instance, early works like BLIP-2[21] introduced Q-Former to efficiently bridge visual and language features. Models like LLaVA fully map pre-trained image features directly into the semantic space, achieving superior performance but at the cost of increased inference complexity. Additionally, some researchers have focused on the resolution limitations of pre-trained image encoders, developing high-resolution encoding strategies to further enhance the

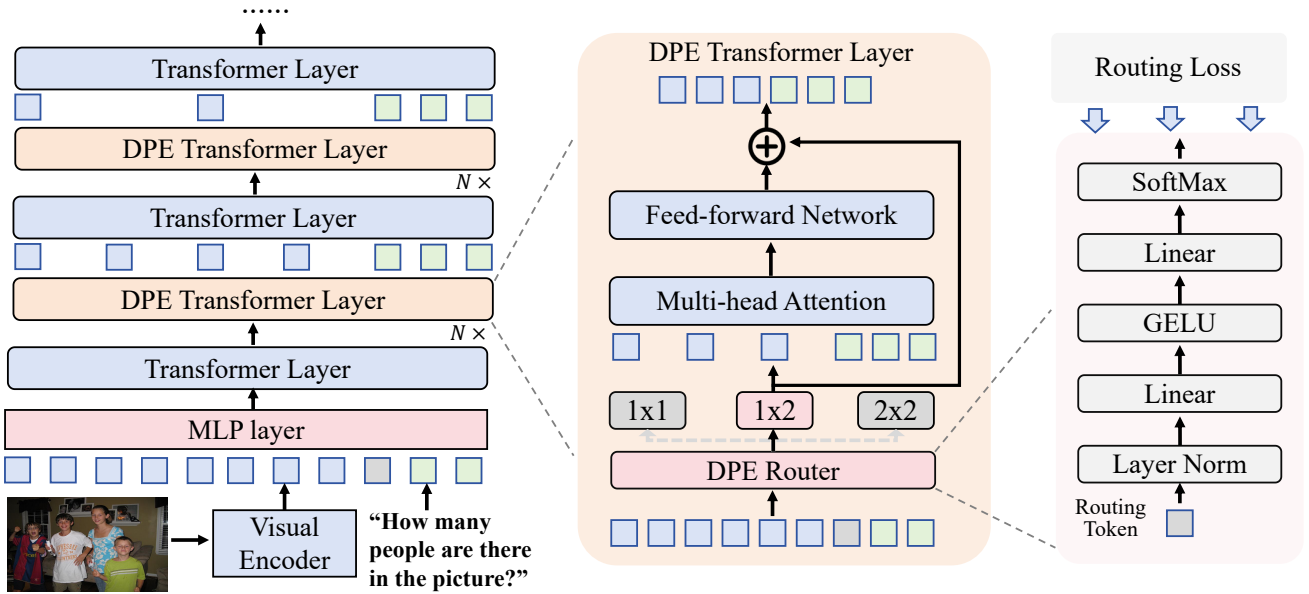


Figure 2. **Illustration of Dynamic Pyramid Network (DPN) and its Dynamic Pooling Experts (DPE).** DPN formulates the common LLM as a dynamic pyramid structure, and the visual tokens will be progressively pooled via the DPE. In practice, DPE can dynamically select an optimal pooling kernel for visual compression, thus achieving the best trade-off between efficiency and performance.

performance of multimodal large language models, as seen in works like LLaVA-HR. However, these high-resolution methods often increase the number of visual tokens, resulting in significantly higher computational costs.

2.3. Efficient Multimodal Large Language Models

Recently, many studies have focused on accelerating multimodal large models, which can be broadly categorized into the exploration of efficient projectors [10, 17, 22, 38, 47] and the investigation of sparse structures [3, 4, 16, 25, 39] within LLMs [6, 26, 34, 45, 46]. Taking the representative work in each direction as an example, Token Packer [22] introduced an efficient projector that only needs to use one-quarter of the original visual tokens. MoE-LLaVA [26] explores sparse structures to reduce the number of activated parameters. FastV [6] discards visual tokens in the LLM middle layer through the attention score. Routing Experts(RoE) [45] allows some tokens to skip complex attention [42] layers and FFN layers through dynamic route prediction. Such methods often have obvious performance degradation in certain types of tasks, and the efficient projector method brings more training costs. Our proposed DPN performs dynamic compression within MLLMs, automatically selecting an appropriate compression ratio based on the complexity of the visual task. This approach maximizes inference efficiency while preserving the model’s ability to perceive image details. In addition, our method provides a simpler training method, which can be integrated

with the visual instruction tuning stage of MLLM and reuse the pre-trained projector, instead of requiring multi-stage training like RoE-LLaVA and MoE-LLaVA.

3. Preliminaries

We first recap the structure of existing MLLMs and their efficient variants.

Plain MLLMs. As shown in Fig 1, existing MLLMs typically adopt the ViT-MLP-LLM structure, *e.g.*, LLaVA [29]. In particular, given the input image $I \in \mathbb{R}^{H \times W \times 3}$, a ViT as visual encoder is used to extract the visual features, denoted by $X \in \mathbb{R}^{(h \times w) \times d}$. After that, the visual features are projected into the embedding space of the LLM via an MLP layer. Finally, the visual features $X \in \mathbb{R}^{(h \times w) \times d}$ are combined with the text features $Y \in \mathbb{R}^{(t-1) \times d}$ and fed into the LLM to decode the words. Therefore, a typical MLLM can be formulated by:

$$p_t = \mathcal{F}_{\text{lm}}(y_t | \mathcal{F}_{\text{proj}}(x; \theta_p), y_{0:t-1}; \theta). \quad (1)$$

Where $y \in Y$ and $p_t \in \mathbb{R}^m$ denote the text features and the next-token probability, respectively. \mathcal{F}_{lm} and $\mathcal{F}_{\text{proj}}$ denote the LLM and the projector, respectively. θ and θ_p are their corresponding parameters. In Eq. 1, we can see that the computation cost of the MLLM is highly dependent on the number of the input features, *i.e.*, $[F_v, F_t]$. In practice, the number of visual features is much longer than that of textual features, *e.g.*, 576 vs. ~ 30 in LLaVA [29].

Efficient Projector. To maintain the model efficiency, numerous works propose the efficient projector to reduce the number of visual features [10, 17, 22, 38]. In particular, given a down-sampling rate k , existing efficient projectors aim to pool the visual features into a smaller shape. In this case, the MLLM can be re-formulated by:

$$p_t = \mathcal{F}_{\text{ilm}}(y_t | \mathcal{F}_{\text{proj}}(x; \theta_p, k), y_{0:t-1}; \theta). \quad (2)$$

As shown in Eq. 2, the projector is placed outside the LLM and its visual compression completely relies on the visual saliency or the pre-defined kernel. Such practices often lead to two potential limitations: 1). Useful visual details will be eliminated before feeding into the LLM. 2). A static compression rate struggles to be optimal for all samples.

4. Dynamic Pyramid Network

4.1. Overview

To overcome the above limitations, we formulate the MLLM as a dynamic pyramid network (DPN). As shown in Fig. 2, the most unique property of DPN lies in that the visual compression module is embedded into the LLM and the compression rate is also dynamically dependent on the input features. Specifically, a DPN layer can be defined by

$$\begin{aligned} Z &= [\mathcal{F}_{\text{dpe}}(x; \theta_d, k_0, k_1, k_2), y], \\ Z &= \text{MHA}(\text{Norm}(Z)) + Z, \\ Z &= \text{FFN}(\text{Norm}(Z)) + Z'. \end{aligned} \quad (3)$$

Here, MHA, FFN, and Norm denote the multi-head attention [42], the feed-forward network [42] and the normalization [41], respectively. $[.]$ is the concatenation operation. \mathcal{F}_{dpe} and θ_d denote the dynamic pooling expert layer, which will dynamically select a pooling kernel from $\{k_0, k_1, k_2\}$ to down-sample the visual features. As shown in Fig. 2, we will replace the 8-th, 16-th and 24-th layers of LLM with our DPN layer, yielding a novel dynamic pyramid structure. Compared with previous studies, such a structure not only prevents fine-grained visual contents in shallow layers, but also maximizes efficiency according to the input samples.

4.2. Dynamic Pooling Experts

The key of Dynamic Pooling Experts (DPE) is to select an optimal visual compression rate based on the given samples, *i.e.*, the visual and textual content. Therefore, we formulated DPE as an mixture-of-expert layer, where each expert is defined as a projection layer with different compression rates. To approach this target, we first insert a learnable routing token $r \in \mathbb{R}^d$ into the input features, *i.e.*, $[x, y, r]$. In this case, the routing token can aggregate the vision-language information of input features through the attention mechanism, thereby making the optimal decision for its routing. In particular, DPE is defined as:

$$\mathcal{F}_{\text{dpe}}(x, r) = R(r)_i E_i(x), \quad (4)$$

where $i = \text{Top}_1(R(r))$ indicates the index with the highest score. $R(\cdot)$ and $E(\cdot)$ denote the router and the pooling expert. In our experiments, the pooling experts can be simply defined as the max pooling layers with a set of pre-defined kernels $\{k_0, k_1, k_2\}$. And the router $R(\cdot)$ can be written as:

$$R(r) = \sigma(\text{MLP}(r)). \quad (5)$$

Here, $\sigma(\cdot)$ is the softmax function. As defined in Eq. 5, the router will predict scores to indicate the significance for each pooling expert. During inference, DPE will select the pooling expert with the highest probability to reduce the number of visual tokens.

4.3. Routing Loss

Routing loss aims to maximize the visual sparsity while encouraging the routing diversity. Without the routing loss, the router will be completely optimized by the autoregressive loss and tends to select a constant expert. To this end, we design the routing loss as a hinge function that can keep the expected compression rate close to our pre-defined target. In this case, the routing loss can be written as:

$$\mathcal{L}_r = \max(0, t - \frac{1}{n} \sum_{i=1}^n R(r)_i C_i), \quad (6)$$

where C_i denotes the compression rate of the i -th pooling expert, *e.g.*, 0.75 for 2×2 pooling. t is the target compression rate, which is set to 0.84 in our experiments.

Therefore, the overall learning objective of the MLLM is

$$\mathcal{L} = \mathcal{L}_a + \lambda \cdot \mathcal{L}_r. \quad (7)$$

Here, \mathcal{L}_a denotes the original autoregressive loss of the MLLM. λ is a coefficient to balance the contribution of two losses, which is set to 0.01 in our experiments.

4.4. The Deployment on MLLMs

Our DPN can be seamlessly deployed on most existing MLLMs, *e.g.*, LLaVA [29] and LLaVA-HR [33]. In existing MLLMs, training is typically divided into two stages, *i.e.*, vision-text alignment and visual instruction tuning. Our DPN is deployed in the instruction tuning stage, and replaces 8-th, 16-th and 24-th standard Transformer layers of the MLLM with our DPE layers. Therefore, we can directly skip the alignment stage by using existing pre-trained weights. During inference, our DPN can directly conduct dynamic inference without any modification.

4.5. Efficiency Analysis

For FLOPs estimation, we follow the calculation method of FastV[6] and only consider the multi-head attention (MHA) layer and feed-forward network (FFN) layer. For one transformer layer, assume n is the token number, d is the hidden state size, m is the intermediate size of FFN, the total

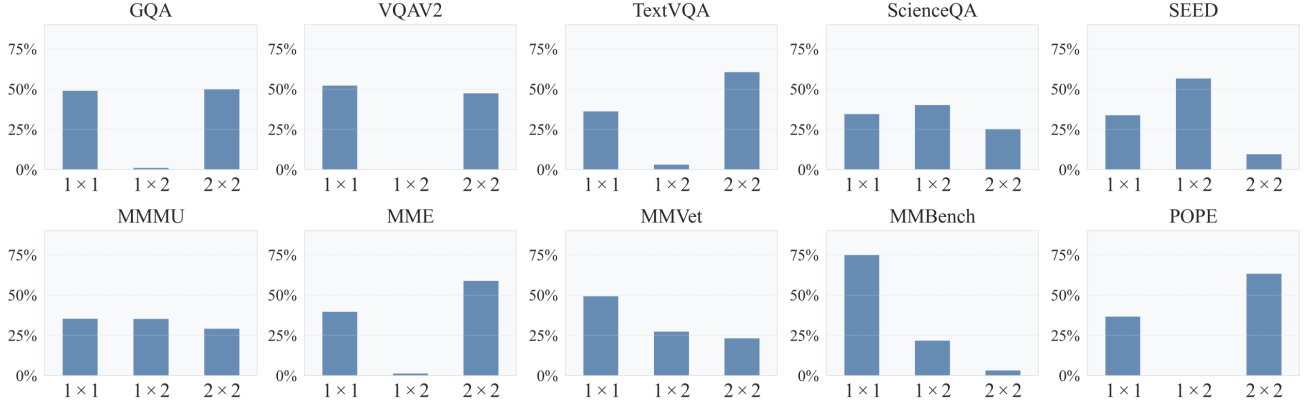


Figure 3. **Statistics of expert activation for different datasets.** our DPN can dynamically select the pooling kernel according to the task difficulty.

FLOPs can be estimated by $4nd^2 + 2n^2d + 2ndm$. Our method will lead to different number of tokens in different layers. Assume n_i is the number of tokens in the i -th layer, the theoretical FLOPs ratio of our method compared to the baseline is computed as:

$$\frac{\sum_{i=1}^I 4n_i d^2 + 2n_i^2 d + 2n_i dm}{I \times (4nd^2 + 2n^2d + 2ndm)}. \quad (8)$$

For the overall FLOPs of our method, we average the single FLOPs value of all samples. In practice, $n_i \ll n$ and the overall FLOPs will be greatly reduced via our DPN.

5. Experiments

5.1. Datasets and Metrics

We test DPN on ten extensive public datasets, including four common vision-language benchmarks, including VQAv2 [13], GQA [14], ScienceQA [32], and TextVQA [40] that evaluate basic object recognition, spatial reasoning, and text reading in images. We report results in their default settings. In addition, we evaluate DPN on six multimodal benchmarks for MLLMs, including MME [12], MMB [30], MM-Vet [50], MMMU [51], SEED [19], POPE [23] that assess broader multimodal comprehension and abstract reasoning. We report all the results in their default settings. For MME, we report the perception score.

5.2. Implementation Details

We validate our method on LLaVA [29] and LLaVA-HR [33] followed by their default settings and reuse their pre-trained image projector from the visual-language alignment stage. In the visual instruction tuning stage, fine-tuning is conducted on LLaVA’s 665K vision instruction dataset [29]; we insert our Dynamic Pooling Experts layer

and train it simultaneously. For the 7B model with 32 transformer layers, we insert DPE after the 8th, 16th, and 24th layers. For the 13B model with 40 transformer layers, we insert DPE after the 10th, 20th, and 30th layers. During fine-tuning, the routing loss ratio is set to 0.01 for LLaVA and 1.0 for LLaVA-HR, depending on the input’s resolution.

5.3. Experimental Results

5.3.1. Ablation Study

We conduct a series of ablation experiments in Table 3 and Table 4 to validate each design in our DPN framework.

First, we examine naive pooling strategies (e.g., pre-pooling or random pooling), which fail on certain benchmarks and substantially degrade performance, confirming that simplistic pooling schedules cannot effectively preserve accuracy. In contrast, our *Dynamic Pooling Experts* (DPE) mechanism adaptively selects the most suitable pooling kernel size at deeper layers, improving GQA by +2.27% and VQA^T by +1.2% over the base model.

We explored the selection of pooling kernel sizes in the first, second, and third rows of Table 3. Using 1×2 max pooling to merge adjacent tokens is an intuitive approach that better aligns with the autoregressive nature of the model. We also experimented with the 2×1 pooling approach, but its overall performance was inferior to that of 1×2 pooling. Since both methods achieve the same acceleration ratio, our final approach adopts dynamic 1×2 and 2×2 pooling.

We also explored larger 4×4 pooling in the 4-th and 5-th rows of Table 3, as well as the insertion of DPE at earlier layers (4th, 8th, and 12th). These modifications slightly impacted performance. We believe that introducing excessive compression during training increases the learning difficulty for the model. Therefore, inserting pooling layers evenly across different model depths and adopting dynamic 1×2 and 2×2 pooling provides better generalization and

Methods	Params	GQA	SQA ^I	VQA ^T	VQA ^{V2}	MME	MM-Vet	MMB	MMMU	SEED ^I	POPE	Avg	FLOPs	Speed
I-80B [18]	65B	45.2	-	-	60.0	-	-	54.5	-	-	-	-	-	-
InstructBLIP [11]	14B	49.5	63.1	50.7	-	1212	25.6	-	-	-	78.9	-	-	-
VILA [27]	7B	62.3	68.2	64.4	79.9	1533	34.9	68.9	-	-	85.5	-	-	-
Qwen-VL[2]	10B	59.3	67.1	63.8	78.8	1487	-	38.2	-	-	-	-	-	5.3
MoE-LLaVA [18]	2.7Bx4	62.5	67.4	64.6	51.4	1423	34.3	65.2	-	-	86.3	62.9	-	6.1
LLaVA 1.5 [29]	7B	62.0	66.8	58.2	78.5	1510	31.1	62.1	35.3	66.2	85.9	65.0	2986	9.3
RoE-LLaVA [45]	7B	61.4	68.4	56.8	80.3	1522	31.9	64.3	-	-	86.1	65.2	2039	9.8
FastV(K=3,R=0.5) [6]	7B	60.4	68.6	45.5	75.8	1510	32.4	63.8	35.2	65.3	85.0	63.4	1431	10.8
FastV(K=3,R=0.6) [6]	7B	59.1	68.5	44.7	75.1	1496	30.2	63.8	36.3	64.4	83.7	62.5	1192	12.3
DPN-LLaVA	7B	63.2	67.7	57.9	79.3	1469	28.7	65.8	36.8	68.4	87.7	65.5	1137	12.7
LLaVA-HR [33]	7B	64.2	67.9	67.1	81.9	1547	31.5	65.0	35.3	64.2	87.6	67.8	5429	5.0
RoE-LLaVA-HR [45]	7B	62.5	67.4	64.6	80.9	1558	30.0	64.6	-	-	88.1	67.0	4940	5.0
DPN-LLaVA-HR	7B	63.9	69.3	65.8	81.5	1471	32.2	64.8	34.6	70.4	88.2	67.4	3257	7.1
LLaVA-HR-X [33]	13B	65.2	69.7	70.9	82.9	1487	40.3	64.5	36.6	71.7	88.8	69.4	10522	2.8
DPN-LLaVA-HR-X	13B	64.6	71.0	70.1	82.9	1473	38.4	66.3	34.4	71.7	90.9	69.7	5892	4.1

Table 1. **Comparison with existing efficient MLLMs.** ‘‘AVG’’ denotes the average performance of all benchmark datasets. The best performance value is highlighted in bold. The speed is the average number of test samples per second and FLOPs is measured in billions.

Methods	#Token	VQA ^{V2}	GQA	POPE	VizWiz	VQA ^T	MMMU	MMB	MME	Avg.
MLP	576	78.5	62.0	85.9	50.0	58.20	35.2	64.3	1510	63.43
Average-Pooling	144	76.2	61.6	86.8	48.0	56.55	34.7	64.3	1443	62.34
Resampler[2]	144	75.1	58.4	84.7	51.9	-	-	63.1	-	-
C-Abstractor[5]	144	74.6	59.2	84.6	49.2	-	-	63.1	-	-
Pixel-Shuffle [7]	144	76.2	60.1	85.9	48.8	-	-	64.0	-	-
LDP-v2 [10]	144	77.3	61.1	86.1	47.6	-	-	66.2	-	-
PruMerge +[38]	~144	76.8	-	84.0	-	57.10	-	60.9	1462	-
TokenPacker [22]	144	77.9	61.8	87.0	52.0	57.16	35.9	65.1	1450	63.68
Ours	~232	79.3	63.2	87.7	51.7	57.93	36.8	65.8	1469	64.48

Table 2. **Comparison with existing projector-based acceleration methods.** Replacing the projector requires more training cost, while our method is simpler and can achieve more stable performance.

performance.

Moreover, when we further incorporate the *Routing Loss*, the FLOPs ratio is reduced from 50% to 39% on GQA, and metrics on MMMU increase by +1.7%. As shown in Table 3, this approach not only stabilizes training but also achieves significant efficiency gains on tasks, where we observe up to -13.4% FLOPs reduction compared to the baseline. Notably, our final design (Dynamic $1 \times 2, 2 \times 2$ Pooling) achieves the highest average performance of 63.29%, surpassing the static 2×2 pooling baseline by +1.21%. These results clearly demonstrate the effectiveness of each proposed component in achieving an excellent trade-off between efficiency and performance.

5.4. Comparison with Existing Methods

As shown in Table 1, we provide a detailed comparison of MLLM deployed by DPN with both dense and sparse models on 10 benchmarks. DPN consistently achieves superior performance across multiple benchmarks while performing as the most efficient method. For example, com-

pared to LLaVA 1.5, DPN-LLaVA (7B) achieves a +1.2% improvement on the GQA benchmark and a +2.2% gain on the POPE metric. Moreover, our approach reduces the required FLOPs by over 50% and boosts the inference speed by more than 36%, clearly demonstrating a better trade-off between performance and efficiency. Table 2 further illustrates the advantages of our method when compared to various efficient projector acceleration techniques, such as MLP, Average-Pooling, and TokenPacker. With approximately 232 tokens, our approach achieves the highest scores in key tasks—for instance, on the VQA^{V2} benchmark, our method records a score of 79.3%, which is +0.8% higher than the closest competitor MLP, and on the GQA task it outperforms MLP methods by around +1.2% while having around 59.7% fewer tokens. These improvements in performance and efficiency, along with simplicity of our training process, further confirm superior performance and efficiency of DPN.

In Figure 4, we further perform a visual analysis comparison with relevant methods to demonstrate that our ap-

Methods	Layers	GQA	VQA ^T	SEED ^I	POPE	MMMU	MMB	Average
static 2×1 pooling	8,16,24	62.34	57.39	66.6	87.1	34.7	64.4	62.08
static 1×2 pooling	8,16,24	62.12	57.70	67.43	87.8	34.6	63.6	62.20
static 2×2 pooling	8,16,24	63.03	57.57	67.43	87.7	33.4	65.0	62.36
dynamic $2 \times 2, 4 \times 4$ pooling	8,16,24	60.72	54.94	62.33	86.4	34.6	59.3	59.72
dynamic $1 \times 2, 2 \times 2$ pooling	4,8,12	59.86	53.92	63.02	85.7	34.4	60.2	59.52
dynamic $1 \times 2, 2 \times 2$ pooling	8,16,24	63.17	57.93	68.36	87.7	36.8	65.8	63.29

Table 3. **Comparison static pyramid network with our DPN.** “Static” denotes that the routing scheme is not used and visual tokens are directly pooled by a constant kernel. “Layers” denotes the placement of the DPE.

Methods	GQA		VQA ^T		POPE		MMMU	
	Metrics	FLOPs Ratio	Metrics	FLOPs Ratio	Metrics	FLOPs Ratio	Metrics	FLOPs Ratio
Baseline	62	100%	58.2	100%	85.9	100%	35.2	100%
+ DPE	63.17	50%	58.4	47%	87.9	48.4%	35.1	40%
+ Routing Loss	63.17	39%	57.93	36%	87.7	35%	36.8	44%

Table 4. **Ablation Study of DPN on LLaVA.** Our baseline is the original LLaVA without any modification.

proach can adjust visual token allocation based on image complexity and task specificity, highlighting its superiority in fine-grained understanding tasks. For instance, in the chart comprehension task shown in the first row of Figure b, existing methods exhibit noticeable errors. When asked, “What is the second step suggested?”, both Fast V and TokenPacker provided incorrect answers, stating “create list of the processes”, whereas our model correctly understood and captured the right response: “identify your audience”. Similarly, in the text recognition task depicted in the second row, other methods also performed poorly, either missing or misidentifying certain characters, while our approach produced accurate results. Additionally, existing methods made errors in the counting task, as seen in the second image of the third row, where six birds were mistakenly identified as five. These errors highlight that direct visual compression or indiscriminate token removal can lead to significant inaccuracies. In contrast, the DPN we propose applies progressive dynamic compression in MLLMs, better preserving their ability to perceive image details.

5.4.1. Quantitative Analysis

The Diversity of Routing. We conducted a statistical analysis of the expert selection process for DPN-LLaVA 1.5 7B across different datasets, as presented in Fig 3. It is important to note that each sample undergoes expert selection three times. For simplicity, we aggregate these selections without distinguishing between layers. Generally, each dataset results in 4 to 7 distinct routing patterns.

The Impact of Image Complexity on Routing. Next, we analyzed the routing tendencies of DPE across various VQA samples, sampling from different routing patterns and visualizing the results in Figure 4. Our observations reveal that

for complex images, DPE tends to avoid pooling. For instance, in the first row, the first image features a variety of fruits and text, prompting minimal pooling. In contrast, for simpler images containing only one or a few primary objects, DPE typically applies a 1×2 pooling, reducing the visual tokens by 50%, as shown in the second picture and third picture in the first row. For even simpler images, such as charts, DPE often utilizes 2×2 pooling, reducing 75% of the visual tokens, as illustrated in the fourth and fifth rows. This behavior is intuitive, as charts contain more structured and densely packed information, making them easier to represent with fewer tokens than photographs.

The Impact of Question Complexity on Routing. Finally, we perform simpler visual tasks on the first and second images of Figure 4 to explore the impact of visual tasks on routing. The results indicate that DPN can recognize simpler visual tasks and perform inference more efficiently.

For the complex fruit image in the first column, the original question likely prompted the model to focus on intricate details, such as identifying specific types of fruit or distinguishing between similarly colored objects. However, when we simplified the question to “Is there any fruit?” the model no longer needed to process such fine-grained information. Instead, it relied on broader, more generalized visual features to determine the presence of fruit. In this case, the DPE model selected a larger kernel size, which allowed it to process larger regions of the image at once. This decision not only reduced the computational load but also improved processing speed, as larger kernels aggregate information more efficiently over wider areas.

In the case of the second image, the original reasoning-based question required extensive contextual information—such as the mood conveyed by the photo, the environ-

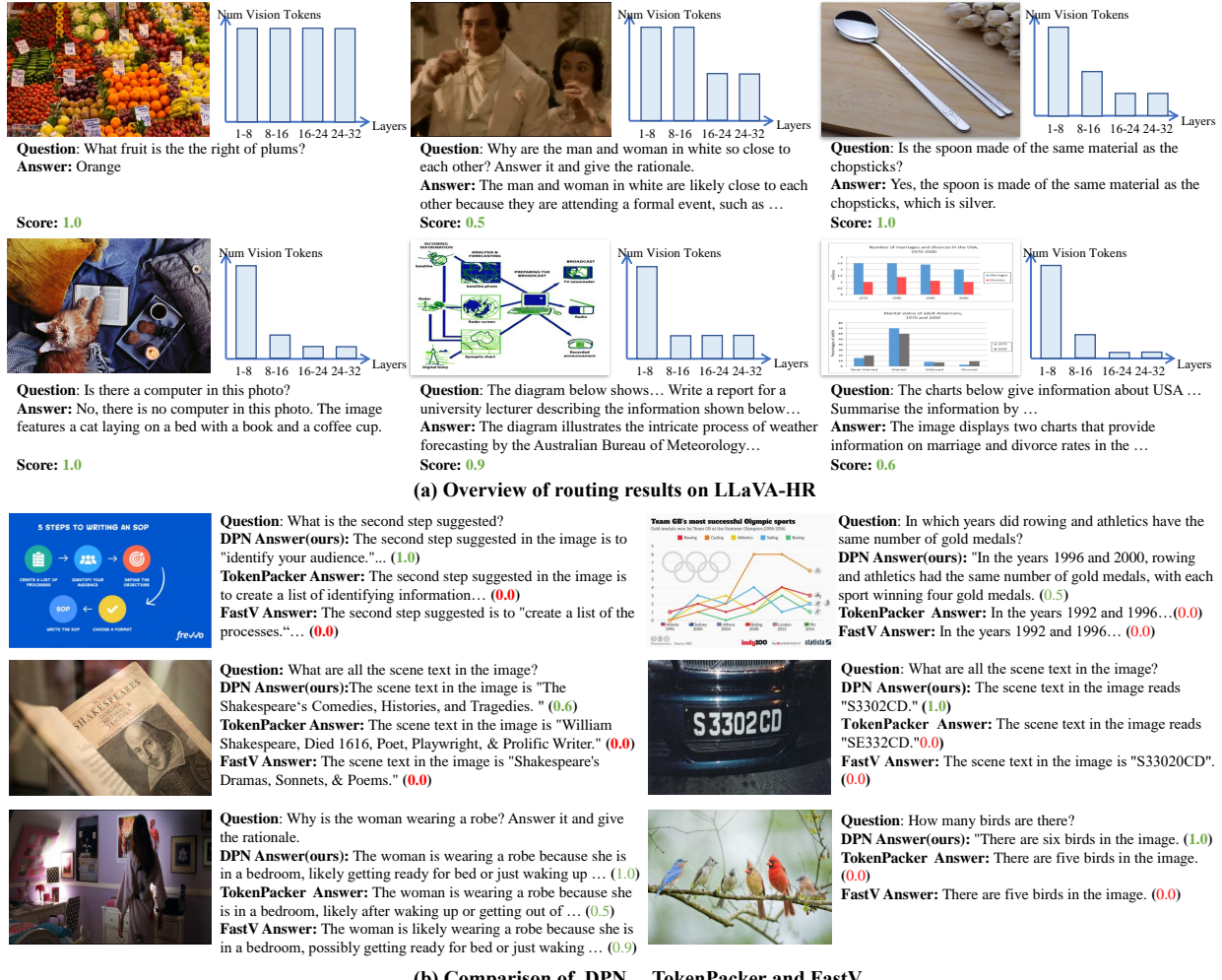


Figure 4. **Visualization Results.** Sub-figure A illustrates the routing of the DPN method across different visual tasks. Sub-figure B presents a visual comparison with the sparsification method FastV and the efficient projector-based approach TokenPacker. Our method demonstrates significant advantages in tasks such as optical character recognition (OCR), chart interpretation, and object detection.

ment, and the clothing and expressions of the individuals. All of these factors influenced the model’s reasoning process. We switched to a simpler counting task, “How many main characters are there in the picture?”, for testing. In this setup, DPN applies a 50% compression in the first and second DPELayer, achieving greater efficiency.

6. Conclusions

Existing acceleration methods, such as sparsification structures in MLLMs or efficient projector-based approaches, often compromise the perceptual capabilities of MLLMs. In this paper, we propose a novel Dynamic Pyramid Network (DPN) designed for efficient MLLMs, in which visual representations undergo progressive dynamic compression as depth increases. Under this framework, even with

a high compression ratio, the model can still capture fine-grained visual details at shallow layers. We introduced Dynamic Pooling Experts (DPE) and Routing Loss to further improve inference efficiency without affecting performance or adding extra training overhead. We verified the necessity of each module design through ablation studies. We conduct extensive experiments on two popular MLLMs and ten benchmarks. The results demonstrate that DPN reduces FLOPs by 56% on LLaVA while achieving a 0.74% performance improvement, outperforming existing methods. Furthermore, the generalization capability of DPN is validated on the high-resolution MLLM LLaVA-HR. We also provide a visual analysis comparing expert routing with related approaches, showing that DPN dynamically selects the optimal visual compression ratio based on input features and shows obvious advantages in various VL tasks.

References

[1] Jinze Bai, Shuai Bai, Yunfei Chu, Zeyu Cui, Kai Dang, Xiaodong Deng, Yang Fan, Wenbin Ge, Yu Han, Fei Huang, Binyuan Hui, Luo Ji, Mei Li, Junyang Lin, Runji Lin, Dayiheng Liu, Gao Liu, Chengqiang Lu, Keming Lu, Jianxin Ma, Rui Men, Xingzhang Ren, Xuancheng Ren, Chuanqi Tan, Sinan Tan, Jianhong Tu, Peng Wang, Shijie Wang, Wei Wang, Shengguang Wu, Benfeng Xu, Jin Xu, An Yang, Hao Yang, Jian Yang, Shusheng Yang, Yang Yao, Bowen Yu, Hongyi Yuan, Zheng Yuan, Jianwei Zhang, Xingxuan Zhang, Yichang Zhang, Zhenru Zhang, Chang Zhou, Jingren Zhou, Xiaohuan Zhou, and Tianhang Zhu. Qwen technical report, 2023. 2

[2] Jinze Bai, Shuai Bai, Shusheng Yang, Shijie Wang, Sinan Tan, Peng Wang, Junyang Lin, Chang Zhou, and Jingren Zhou. Qwen-vl: A versatile vision-language model for understanding, localization, text reading, and beyond, 2023. 1, 6

[3] Daniel Bolya, Cheng-Yang Fu, Xiaoliang Dai, Peizhao Zhang, Christoph Feichtenhofer, and Judy Hoffman. Token merging: Your vit but faster, 2023. 3

[4] Qingqing Cao, Bhargavi Paranjape, and Hannaneh Hajishirzi. Pumer: Pruning and merging tokens for efficient vision language models, 2023. 3

[5] Junbum Cha, Wooyoung Kang, Jonghwan Mun, and Byungseok Roh. Honeybee: Locality-enhanced projector for multimodal llm, 2024. 6

[6] Liang Chen, Haozhe Zhao, Tianyu Liu, Shuai Bai, Junyang Lin, Chang Zhou, and Baobao Chang. An image is worth 1/2 tokens after layer 2: Plug-and-play inference acceleration for large vision-language models, 2024. 1, 3, 4, 6

[7] Zhe Chen, Weiyun Wang, Hao Tian, Shenglong Ye, Zhangwei Gao, Erfei Cui, Wenwen Tong, Kongzhi Hu, Jiapeng Luo, Zheng Ma, Ji Ma, Jiaqi Wang, Xiaoyi Dong, Hang Yan, Hewei Guo, Conghui He, Botian Shi, Zhenjiang Jin, Chao Xu, Bin Wang, Xingjian Wei, Wei Li, Wenjian Zhang, Bo Zhang, Pinlong Cai, Licheng Wen, Xiangchao Yan, Min Dou, Lewei Lu, Xizhou Zhu, Tong Lu, Dahua Lin, Yu Qiao, Jifeng Dai, and Wenhui Wang. How far are we to gpt-4? closing the gap to commercial multimodal models with open-source suites, 2024. 6

[8] Wei-Lin Chiang, Zhuohan Li, Zi Lin, Ying Sheng, Zhang-hao Wu, Hao Zhang, Lianmin Zheng, Siyuan Zhuang, Yong-hao Zhuang, Joseph E. Gonzalez, Ion Stoica, and Eric P. Xing. Vicuna: An open-source chatbot impressing gpt-4 with 90%* chatgpt quality, 2023. 2

[9] Xiangxiang Chu, Limeng Qiao, Xinyang Lin, Shuang Xu, Yang Yang, Yiming Hu, Fei Wei, Xinyu Zhang, Bo Zhang, Xiaolin Wei, and Chunhua Shen. Mobilevlm : A fast, strong and open vision language assistant for mobile devices, 2023. 1, 2

[10] Xiangxiang Chu, Limeng Qiao, Xinyu Zhang, Shuang Xu, Fei Wei, Yang Yang, Xiaofei Sun, Yiming Hu, Xinyang Lin, Bo Zhang, and Chunhua Shen. Mobilevlm v2: Faster and stronger baseline for vision language model, 2024. 1, 3, 4, 6

[11] Wenliang Dai, Junnan Li, Dongxu Li, Anthony Meng Huat Tiong, Junqi Zhao, Weisheng Wang, Boyang Li, Pascale Fung, and Steven Hoi. Instructblip: Towards general-purpose vision-language models with instruction tuning, 2023. 1, 2, 6

[12] Chaoyou Fu, Peixian Chen, Yunhang Shen, Yulei Qin, Mengdan Zhang, Xu Lin, Jinrui Yang, Xiaowu Zheng, Ke Li, Xing Sun, Yunsheng Wu, and Rongrong Ji. Mme: A comprehensive evaluation benchmark for multimodal large language models, 2024. 1, 5

[13] Yash Goyal, Tejas Khot, Douglas Summers-Stay, Dhruv Batra, and Devi Parikh. Making the v in vqa matter: Elevating the role of image understanding in visual question answering, 2017. 5

[14] Drew A. Hudson and Christopher D. Manning. Gqa: A new dataset for real-world visual reasoning and compositional question answering, 2019. 1, 5

[15] Albert Q. Jiang, Alexandre Sablayrolles, Antoine Roux, Arthur Mensch, Blanche Savary, Chris Bamford, Devendra Singh Chaplot, Diego de las Casas, Emma Bou Hanna, Florian Bressand, Gianna Lengyel, Guillaume Bour, Guillaume Lample, Lélio Renard Lavaud, Lucile Saulnier, Marie-Anne Lachaux, Pierre Stock, Sandeep Subramanian, Sophia Yang, Szymon Antoniak, Teven Le Scao, Théophile Gervet, Thibaut Lavril, Thomas Wang, Timothée Lacroix, and William El Sayed. Mixtral of experts, 2024. 2

[16] Zhenglun Kong, Peiyan Dong, Xiaolong Ma, Xin Meng, Mengshu Sun, Wei Niu, Xuan Shen, Geng Yuan, Bin Ren, Minghai Qin, Hao Tang, and Yanzhi Wang. Sput: Enabling faster vision transformers via soft token pruning, 2022. 3

[17] Zhibin Lan, Liqiang Niu, Fandong Meng, Wenbo Li, Jie Zhou, and Jinsong Su. Avg-llava: A large multimodal model with adaptive visual granularity, 2024. 3, 4

[18] Hugo Laurençon, Lucile Saulnier, Léo Tronchon, Stas Bekerman, Amanpreet Singh, Anton Lozhkov, Thomas Wang, Siddharth Karamcheti, Alexander M. Rush, Douwe Kiela, Matthieu Cord, and Victor Sanh. Obelics: An open web-scale filtered dataset of interleaved image-text documents, 2023. 6

[19] Bohao Li, Rui Wang, Guangzhi Wang, Yuying Ge, Yixiao Ge, and Ying Shan. Seed-bench: Benchmarking multimodal llms with generative comprehension. *arXiv preprint arXiv:2307.16125*, 2023. 1, 5

[20] Bo Li, Yuanhan Zhang, Dong Guo, Renrui Zhang, Feng Li, Hao Zhang, Kaichen Zhang, Peiyuan Zhang, Yanwei Li, Ziwei Liu, and Chunyuan Li. Llava-onevision: Easy visual task transfer, 2024. 1, 2

[21] Junnan Li, Dongxu Li, Silvio Savarese, and Steven Hoi. Blip-2: Bootstrapping language-image pre-training with frozen image encoders and large language models, 2023. 2

[22] Wentong Li, Yuqian Yuan, Jian Liu, Dongqi Tang, Song Wang, Jie Qin, Jianke Zhu, and Lei Zhang. Tokenpacker: Efficient visual projector for multimodal llm, 2024. 1, 3, 4, 6

[23] Yifan Li, Yifan Du, Kun Zhou, Jinpeng Wang, Wayne Xin Zhao, and Ji-Rong Wen. Evaluating object hallucination in large vision-language models. In *The 2023 Conference on Empirical Methods in Natural Language Processing*, 2023. 1, 5

[24] Yanwei Li, Yuechen Zhang, Chengyao Wang, Zhisheng Zhong, Yixin Chen, Ruihang Chu, Shaoteng Liu, and Jiaya Jia. Mini-gemini: Mining the potential of multi-modality vision language models, 2024. 1, 2

[25] Youwei Liang, Chongjian Ge, Zhan Tong, Yibing Song, Jue Wang, and Pengtao Xie. Not all patches are what you need: Expediting vision transformers via token reorganizations, 2022. 3

[26] Bin Lin, Zhenyu Tang, Yang Ye, Jiaxi Cui, Bin Zhu, Peng Jin, Jinfa Huang, Junwu Zhang, Yatian Pang, Munan Ning, and Li Yuan. Moe-llava: Mixture of experts for large vision-language models, 2024. 1, 3

[27] Ji Lin, Hongxu Yin, Wei Ping, Yao Lu, Pavlo Molchanov, Andrew Tao, Huizi Mao, Jan Kautz, Mohammad Shoeybi, and Song Han. Vila: On pre-training for visual language models, 2024. 1, 2, 6

[28] Tsung-Yi Lin, Piotr Dollár, Ross Girshick, Kaiming He, Bharath Hariharan, and Serge Belongie. Feature pyramid networks for object detection, 2017. 2

[29] Haotian Liu, Chunyuan Li, Qingyang Wu, and Yong Jae Lee. Visual instruction tuning, 2023. 1, 2, 3, 4, 5, 6

[30] Yuan Liu, Haodong Duan, Yuanhan Zhang, Bo Li, Songyang Zhang, Wangbo Zhao, Yike Yuan, Jiaqi Wang, Conghui He, Ziwei Liu, Kai Chen, and Dahu Lin. Mmbench: Is your multi-modal model an all-around player?, 2024. 1, 5

[31] Ze Liu, Yutong Lin, Yue Cao, Han Hu, Yixuan Wei, Zheng Zhang, Stephen Lin, and Baining Guo. Swin transformer: Hierarchical vision transformer using shifted windows, 2021. 2

[32] Pan Lu, Swaroop Mishra, Tony Xia, Liang Qiu, Kai-Wei Chang, Song-Chun Zhu, Oyvind Tafjord, Peter Clark, and Ashwin Kalyan. Learn to explain: Multimodal reasoning via thought chains for science question answering, 2022. 1, 5

[33] Gen Luo, Yiyi Zhou, Yuxin Zhang, Xiaowu Zheng, Xiaoshuai Sun, and Rongrong Ji. Feast your eyes: Mixture-of-resolution adaptation for multimodal large language models, 2024. 1, 2, 4, 5, 6

[34] Yixin Luo, Gen Luo, Jiayi Ji, Yiyi Zhou, Xiaoshuai Sun, Zhiqiang Shen, and Rongrong Ji. γ -mod: Exploring mixture-of-depth adaptation for multimodal large language models, 2024. 3

[35] OpenAI, Josh Achiam, Steven Adler, Sandhini Agarwal, Lama Ahmad, Ilge Akkaya, Florencia Leoni Aleman, Diogo Almeida, Janko Altenschmidt, Sam Altman, Shyamal Anadkat, Red Avila, Igor Babuschkin, Suchir Balaji, Valerie Balcom, Paul Baltescu, Haiming Bao, Mohammad Bavarian, Jeff Belgum, Irwan Bello, Jake Berdine, Gabriel Bernadett-Shapiro, Christopher Berner, Lenny Bogdonoff, Oleg Boiko, Madelaine Boyd, Anna-Luisa Brakman, Greg Brockman, Tim Brooks, Miles Brundage, Kevin Button, Trevor Cai, Rosie Campbell, Andrew Cann, Brittany Carey, Chelsea Carlson, Rory Carmichael, Brooke Chan, Che Chang, Fotis Chantzis, Derek Chen, Sully Chen, Ruby Chen, Jason Chen, Mark Chen, Ben Chess, and Chester Cho. Gpt-4 technical report, 2024. 2

[36] K O’Shea. An introduction to convolutional neural networks. *arXiv preprint arXiv:1511.08458*, 2015. 2

[37] Alec Radford, Jong Wook Kim, Chris Hallacy, Aditya Ramesh, Gabriel Goh, Sandhini Agarwal, Girish Sastry, Amanda Askell, Pamela Mishkin, Jack Clark, Gretchen Krueger, and Ilya Sutskever. Learning transferable visual models from natural language supervision, 2021. 2

[38] Yuzhang Shang, Mu Cai, Bingxin Xu, Yong Jae Lee, and Yan Yan. Llava-prumerge: Adaptive token reduction for efficient large multimodal models, 2024. 1, 3, 4, 6

[39] Dachuan Shi, Chaofan Tao, Anyi Rao, Zhendong Yang, Chun Yuan, and Jiaqi Wang. Crossget: Cross-guided ensemble of tokens for accelerating vision-language transformers, 2024. 3

[40] Amanpreet Singh, Vivek Natarajan, Meet Shah, Yu Jiang, Xinlei Chen, Dhruv Batra, Devi Parikh, and Marcus Rohrbach. Towards vqa models that can read, 2019. 1, 5

[41] Hugo Touvron, Thibaut Lavril, Gautier Izacard, Xavier Martinet, Marie-Anne Lachaux, Timothée Lacroix, Baptiste Rozière, Naman Goyal, Eric Hambro, Faisal Azhar, Aurelien Rodriguez, Armand Joulin, Edouard Grave, and Guillaume Lample. Llama: Open and efficient foundation language models, 2023. 2, 4

[42] Ashish Vaswani, Noam Shazeer, Niki Parmar, Jakob Uszkoreit, Llion Jones, Aidan N. Gomez, Łukasz Kaiser, and Illia Polosukhin. Attention is all you need, 2023. 2, 3, 4

[43] Peng Wang, Shuai Bai, Sinan Tan, Shijie Wang, Zhihao Fan, Jinze Bai, Keqin Chen, Xuejing Liu, Jialin Wang, Wenbin Ge, Yang Fan, Kai Dang, Mengfei Du, Xuancheng Ren, Rui Men, Dayiheng Liu, Chang Zhou, Jingren Zhou, and Junyang Lin. Qwen2-vl: Enhancing vision-language model’s perception of the world at any resolution, 2024. 2

[44] Wenhui Wang, Enze Xie, Xiang Li, Deng-Ping Fan, Kaitao Song, Ding Liang, Tong Lu, Ping Luo, and Ling Shao. Pyramid vision transformer: A versatile backbone for dense prediction without convolutions, 2021. 2

[45] Qiong Wu, Zhaoxi Ke, Yiyi Zhou, Gen Luo, Xiaoshuai Sun, and Rongrong Ji. Routing experts: Learning to route dynamic experts in multi-modal large language models, 2024. 1, 3, 6

[46] Long Xing, Qidong Huang, Xiaoyi Dong, Jiajie Lu, Pan Zhang, Yuhang Zang, Yuhang Cao, Conghui He, Jiaqi Wang, Feng Wu, et al. Pyramiddrop: Accelerating your large vision-language models via pyramid visual redundancy reduction. *arXiv preprint arXiv:2410.17247*, 2024. 1, 3

[47] Yizhe Xiong, Hui Chen, Tianxiang Hao, Zijia Lin, Jun-gong Han, Yuesong Zhang, Guoxin Wang, Yongjun Bao, and Guiguang Ding. Pyra: Parallel yielding re-activation for training-inference efficient task adaptation, 2024. 3

[48] Ruyi Xu, Yuan Yao, Zonghao Guo, Junbo Cui, Zanlin Ni, Chunjiang Ge, Tat-Seng Chua, Zhiyuan Liu, Maosong Sun, and Gao Huang. Llava-uhd: an lmm perceiving any aspect ratio and high-resolution images, 2024. 1, 2

[49] An Yang, Baosong Yang, Binyuan Hui, Bo Zheng, Bowen Yu, Chang Zhou, Chengpeng Li, Chengyuan Li, Dayiheng Liu, Fei Huang, Guanting Dong, Haoran Wei, Huan Lin, Jialong Tang, Jialin Wang, Jian Yang, Jianhong Tu, Jianwei Zhang, Jianxin Ma, Jianxin Yang, Jin Xu, Jingren Zhou, Jinze Bai, Jinzheng He, Junyang Lin, Kai Dang, Keming Lu,

Keqin Chen, Kexin Yang, Mei Li, Mingfeng Xue, Na Ni, Pei Zhang, Peng Wang, Ru Peng, Rui Men, Ruize Gao, Runji Lin, Shijie Wang, Shuai Bai, Sinan Tan, Tianhang Zhu, Tianhao Li, Tianyu Liu, Wenbin Ge, Xiaodong Deng, Xiaohuan Zhou, Xingzhang Ren, Xinyu Zhang, Xipin Wei, Xuancheng Ren, Xuejing Liu, Yang Fan, Yang Yao, Yichang Zhang, Yu Wan, Yunfei Chu, Yuqiong Liu, Zeyu Cui, Zhenru Zhang, Zhifang Guo, and Zhihao Fan. Qwen2 technical report, 2024.

[2](#)

- [50] Weihao Yu, Zhengyuan Yang, Linjie Li, Jianfeng Wang, Kevin Lin, Zicheng Liu, Xinchao Wang, and Lijuan Wang. Mm-vet: Evaluating large multimodal models for integrated capabilities, 2023. [1](#), [2](#), [5](#)
- [51] Xiang Yue, Yuansheng Ni, Kai Zhang, Tianyu Zheng, Ruoji Liu, Ge Zhang, Samuel Stevens, Dongfu Jiang, Weiming Ren, Yuxuan Sun, Cong Wei, Botao Yu, Ruibin Yuan, Renliang Sun, Ming Yin, Boyuan Zheng, Zhenzhu Yang, Yibo Liu, Wenhao Huang, Huan Sun, Yu Su, and Wenhui Chen. Mmmu: A massive multi-discipline multimodal understanding and reasoning benchmark for expert agi. In *Proceedings of CVPR*, 2024. [1](#), [5](#)